INTERNATIONAL UNION OF PURE AND APPLIED CHEMISTRY

PHYSICAL AND BIOPHYSICAL CHEMISTRY DIVISION*

PRACTICAL GUIDE TO MEASUREMENT AND INTERPRETATION OF MAGNETIC PROPERTIES

(IUPAC Technical Report)

Prepared for publication by
S. HATSCHER[1], H. SCHILDER[2], H. LUEKEN[3,‡], AND W. URLAND[1,‡]

[1]*Institut für Anorganische Chemie, Universität Hannover, Callinstrasse 9, 30167 Hannover, Germany;* [2]*Fachbereich Chemieingenieurwesen der Fachhochschule Aachen, Kalverbenden 6, 52066 Aachen, Germany;* [3]*Institut für Anorganische Chemie, Rheinisch-Westfälische Technische Hochschule Aachen, Professor-Pirlet-Strasse 1, 52074 Aachen, Germany*

‡Corresponding authors: E-mail: Heiko.Lueken@ac.rwth-aachen.de; Urland@acc.uni-hannover.de

Practical guide to measurement and interpretation of magnetic properties

(IUPAC Technical Report)

Abstract: Rules are pointed out to protect the magnetochemist from pitfalls in both measurement and interpretation of magnetic data. Carefully chosen magnetic field strengths during magnetic susceptibility measurements guarantee the recording of genuine data. With the help of examples, the effect of too strong applied fields is demonstrated producing magnetic saturation and, for example, quenching of weak ferro- or antiferromagnetic spin–spin couplings. In consequence, the data run the risk of being misinterpreted unless model susceptibility equations are applied that take the field dependence of χ_m into consideration. Recommendations are given for the presentation of experimental and theoretical data. The limited applicability of the **most overworked** formula in paramagnetism, the Curie–Weiss law $\chi_m = C/(T-\theta)$, is clearly presented (magnetically condensed systems, pure spin magnetism). While rough and ready susceptibility formulae are applicable to specific 3d and 4f systems, the complex situation for the remaining d and f centers, including actinides, demands computer programs which consider simultaneously interelectronic repulsion, ligand field potential, spin-orbit coupling, interatomic exchange interactions, and applied magnetic field.

Keywords: magnetic properties; magnetochemistry; SQUID magnetometers; Curie–Weiss law; paramagnetism; Division I.

CONTENTS

1. INTRODUCTION

In today's magnetochemistry, superconducting quantum interference device (SQUID) magnetometers [1] are widely used. Automated measurements of high accuracy are state of the art and have the aim to fully characterize magnetic properties of compounds and materials. The findings serve to determine electronic configuration of the magnetic center, interatomic exchange interactions, diamagnetic contributions, metallic character, superconductivity, spin-glass behavior, superparamagnetism, etc. To take

full advantage of experimental data, special attention should be given to: (i) appropriate units, (ii) purity of the sample, (iii) measurement conditions, (iv) suitable graphical presentation of the results, and (v) adequate models. Our practical guide collects subjects which should be taken into consideration in order to present reliable magnetochemical results in a standardized way, to allow correct statements about the electronic structure of the substance under investigation, and to allow comparison between measurements. We presuppose that the reader is familiar with the basic laws and terminology of magnetochemistry.

2. MAGNETIC QUANTITIES AND UNITS

Two principal systems of electromagnetic units are used in magnetochemistry, which can be called "rational" (the SI system) and "irrational" (here, the CGS-emu system), following ref. [2]. In this report, we summarize the relevant relations in both systems, but suggest the use of quantities that lead to values independent of the two systems: (i) the effective Bohr magneton number μ_{eff}; (ii) the magnetic dipole moment $\boldsymbol{m}$ and the atomic magnetic dipole moment μ_a, each divided by the Bohr magneton μ_B ($\boldsymbol{m}/\mu_B$ and μ_a/μ_B, respectively). The frequently used quantities are collected in Table 1 together with conversion factors.

   It is pointed out that the magnetic susceptibility, χ, although dimensionless, converts by the factor 4π; i.e., $\chi = 4\pi\chi^{(ir)}$. Similarly, the magnetic field strengths are related by $\boldsymbol{H}^{(ir)} = 4\pi\boldsymbol{H}$, and the units are related by Oe $= 10^3/4\pi$ A m^{-1}. To avoid the latter inconvenience, we recommend that one use, for example, in graphs $\boldsymbol{B}_0 = \mu_0 \boldsymbol{H}$ (loosely called "magnetic field" [2]) with conversion factor 10^{-4} T/G.

Table 1 Definitions, units, and conversion factors [3,4] (cf. Table 5 for physical constants).

	Quantity	SI	CGS-emu	Factor[a]
μ_0	Permeability of vacuum	$\mu_0 =$ $4\pi \times 10^{-7}$ H/m[b]	1	
$\boldsymbol{B}$	Magnetic induction	$\boldsymbol{B} = \mu_0(\boldsymbol{H} + \boldsymbol{M})$ T $=$ V s/m^2	$\boldsymbol{B} = \boldsymbol{H}^{(ir)} + 4\pi\boldsymbol{M}$ G	10^{-4} T/G
$\boldsymbol{H}$	Magnetic field strength	$\boldsymbol{H}$ A/m	Oe	10^3 Oe $/4\pi$ A m-1
$\boldsymbol{B}_0$	"Magnetic field"	$\boldsymbol{B}_0 = \mu_0 \boldsymbol{H}$ T $=$ V s/m^2	G	10^{-4} T/G
$\boldsymbol{M}$	Magnetization	$\boldsymbol{M}$ A/m	G	10^3 (A/m)/G
$\boldsymbol{m}$	Magnetic dipole moment	$\boldsymbol{m} = \boldsymbol{M}V$ A m^2 = J/T	$\boldsymbol{m} = \boldsymbol{M}V$ G cm^3	10^{-3} A m^2/G cm^3
$\boldsymbol{m}/\mu_B$		1	1	1
μ_B	Bohr magneton	$\mu_B = e\hbar/2m_e$ A m^2	$\mu_B = e\hbar/2m_e$ G cm^3	10^{-3} A m^2/G cm^3
σ	Specific magnetic dipole moment[d]	$\sigma = \boldsymbol{M}/\rho$[c] A m^2/kg	$\sigma = \boldsymbol{M}/\rho$ G cm^3/g	1 (A m^2/kg)/(G cm^3/g)
$\boldsymbol{M}_m$	Molar magnetization[f]	$\boldsymbol{M}_m = \boldsymbol{M} M/\rho$[e] A m^2/mol	$\boldsymbol{M}_m = \boldsymbol{M} M/\rho$ G cm^3/mol	10^{-3} A m^2/G cm^3
μ_a[g]	Atomic magnetic dipole moment	$\mu_a = \boldsymbol{M}_m/N_A$ A m^2	$\mu_a = \boldsymbol{M}_m/N_A$ G cm^3	
μ_a/μ_B		1	1	1
χ	Magnetic volume susceptibility	$\boldsymbol{M} = \chi \boldsymbol{H}$ 1	$\boldsymbol{M} = \chi^{(ir)}\boldsymbol{H}^{(ir)}$ 1	4π
χ_g	Magnetic mass susceptibility	$\chi_g = \chi/\rho$ m^3/kg	$\chi_g^{(ir)} = \chi^{(ir)}/\rho$ cm^3/g	$4\pi/10^3$ (m^3/kg)/(cm^3/g)

(continues on next page)

Table 1 (Continued).

	Quantity	SI	CGS-emu	Factor[a]
χ_m	Molar magnetic susceptibility	$\chi_m = \chi M/\rho$ m^3/mol	$\chi_m^{(ir)} = \chi^{(ir)}M/\rho$ cm^3/mol	$4\pi/10^6\ m^3/cm^3$
μ_{eff}	Effective Bohr magneton number [5]	$[3k_B/\mu_o N_A \mu_B^2]^{1/2}\ [\chi_m T]^{1/2}$ 1	$[3k_B/N_A \mu_B^2]^{1/2}\ [\chi_m T]^{1/2}$ 1	1

[a]Multiplicative factor applied to the value in CGS-emu units to obtain the value in SI units.
[b]H = Henry; H/m = Vs/Am.
[c]ρ = mass density.
[d]Specific magnetization; σ^s = specific saturation magnetization.
[e]M = molar mass.
[f]M_m^s = molar saturation magnetization.
[g]μ_a^s = atomic magnetic saturation moment.

3. SAMPLES AND MEASUREMENTS

In order to yield correct data sets, one has to pay attention to samples and measurement conditions.

3.1 Samples

Generally, only small amounts of substances are necessary for the measurements owing to the high sensitivity of SQUID magnetometers. The precision of weighing the (possibly reactive) sample may then be responsible for the precision of the final data. An ultra-microbalance and a controlled encapsulation of air-sensitive substances in tiny tubes made, for example, of synthetic quartz glass, are necessary preconditions for reliable experimental data. Furthermore, the sample holder contribution to the measured data must be known with high accuracy. If polycrystalline materials are investigated, which is most often the case, one has to pulverize the crystals to such an extent that preferential orientation and movement of the crystals during the measurements are avoided, but magnetic cooperative effects are not destroyed [6].

   Ferromagnetic impurities even in low concentration may affect seriously the precision of the susceptibility values. They are detected by field-dependent measurements and, if it so happens, are arithmetically corrected using the $\chi_g (H) = \chi_g (\infty) + \sigma^s/H$ vs. H^{-1} plot, where $\chi_g(\infty)$ is the mass susceptibility of the pure sample and σ^s the specific saturation magnetization of the impurity. However, one has to beware of too strong applied fields on account of saturation with regard to the compound under investigation (see Section 3.2). Paramagnetic mononuclear impurities are a problem in corresponding polynuclear compounds, especially in the case of antiferromagnetically coupled centers where the susceptibility maximum may be obscured. Diamagnetic impurities in paramagnetic samples cause an error in the weighed portion. In consequence, too small values of susceptibility are obtained for the compound under investigation.

3.2 Measurement conditions

To calibrate the SQUID magnetometer with respect to applied field and temperature, the reference compounds given in Table 2 have proved a success. With regard to the recording of magnetization, valuable instructions are given in ref. [10].

Table 2 Materials for calibration and controlling of magnetometers.

Substance	Control of	Quantity	Value SI (CGS-emu)	Ref.
$HgCo(NCS)_4$	H	χ_g (293 K)	$20.70(6) \times 10^{-8}$ m^3 kg^{-1} $[16.47(5) \times 10^{-6}$ cm^3 g$^{-1}]$	[7]
$(NH_4)_2Mn(SO_4)_2 \cdot 6H_2O$	T	C^a	5.498×10^{-5} m^3 K mol^{-1} (4.375 cm^3 K mol^{-1})	[8]
Pb, In	T	$T_C{}^b$	7.199 9 K, 3.414 6 K	[9]

[a]Curie constant $C = [\mu_0 N_A \mu_B{}^2/3k_B]g^2 S(S + 1)$ with $g = 2$ corresponding to pure spin paramagnetism (cf. eq. 1).
[b]Superconducting transition temperature.

The strength of the applied magnetic field should be chosen carefully. On the one hand, the field should be strong enough to produce well signals that can be evaluated readily. On the other hand, too strong a field may affect considerably the susceptibility data leading to magnetic saturation and distortion of weak electronic couplings. Magnetic saturation plays a role if the condition $\mu_a{}^s B_0/k_B T \ll 1$ [11] is not fulfilled, which is the case, for example, for Gd^{3+} ions at $B_0 > 0.2$ T if T falls below 10 K. With regard to interatomic spin–spin couplings in the cm^{-1} range, one should consider that an external magnetic field $B_0 = 1$ T corresponds to the energy equivalent wavenumber 0.466 864 cm^{-1} (see Appendix), so that spin–spin coupling and applied field have to be regarded as competing effects. Neglecting in these situations the effect of the external field, namely, applying according to common practice a model susceptibility equation which presupposes field-independent data, wrong conclusions are arrived at: (i) magnetic saturation may then falsely be explained by antiferromagnetic interactions and (ii) weak ferro- or antiferromagnetic spin–spin couplings will not be recognized because characteristic features in the $\chi_m - T$ behavior, for example, a steep increase on cooling or a maximum, are quenched by a too strong applied field. Two examples may demonstrate that danger of misinterpretation is ahead.

Situation (i) (see Fig. 1, solid lines) refers to a heterodinuclear Gd(III)–Cu(II) complex ($S_{Gd} = 7/2$, $S_{Cu} = 1/2$) of ferromagnetically coupled spins with the exchange parameter $J_{ex} = 5$ cm^{-1} (spin Hamiltonian for isotropic coupling (Heisenberg model) $\hat{H}_{ex} = -2J_{ex}\,\hat{S}_{Gd}\cdot\hat{S}_{Cu}$). Solely for $B_0 = 0.01$ T (a) the expected plateau at $\mu_{eff} = 8.94$ [12] is obtained at $T \leq 2$ K except for $T \leq 0.2$ K. In order to adjust J_{ex} by fitting procedures to corresponding experimental data, it is justified to apply a susceptibility equation valid for $B_0 \to 0$ (Van Vleck approach). For measurements with the stronger field 0.1 T (b) and all the more 1 T (c) deviations are obvious, which are not adequately described by the simple model. They could be misinterpreted, however, as an additional antiferromagnetic intermolecular spin–spin coupling. A similar problem arises if a corresponding uncoupled system is considered (Fig. 1, dotted lines). A straight line parallel to the T axis is obtained at $\mu_{eff} = 8.13$ [12] for $B_0 \to 0$ (curve a), while increasing deviations from this reference line to lower values are again obvious with increasing field (b,c), falsely interpreted as an intramolecular spin–spin coupling of antiferromagnetic nature. Hence, either the measurements are carried out at very weak applied fields or the extended susceptibility formula is used as in the given model calculations [6,13].
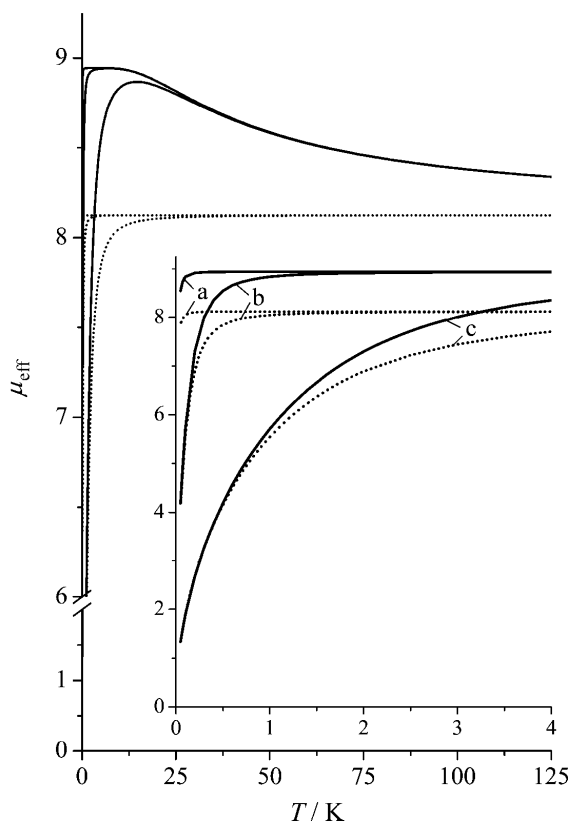
Fig. 1 Calculated μ_{eff} vs. T plots of a ferromagnetically coupled and an uncoupled Gd(III)–Cu(II) unit as a function of the applied field; J_{ex} = 5 cm^{-1} (solid lines), J_{ex} = 0 (dotted lines); g_{Gd} = g_{Cu} = 2; $\boldsymbol{B}_0$ = 0.01 (a), 0.1 (b), 1.0 T (c).

Situation (ii) refers to an antiferromagnetically coupled Cu(II)–Cu(II) unit (S_1 = S_2 = 1/2). Figure 2 exhibits the variation of the energy of the spin states, and Fig. 3 shows the expected variation χ_m vs. T. It is obvious that the position of the susceptibility maximum depends on the applied field strength and the maximum may even disappear according to the change of the $|S'\ M_{S'}\rangle$ ground state with increasing $\boldsymbol{B}_0$ ($|0\ 0\rangle$ for $\boldsymbol{B}_0 \leq 4.3$ T, $|1\ -1\rangle$ for $\boldsymbol{B}_0 \geq 4.5$ T). Similar to the preceding example, for
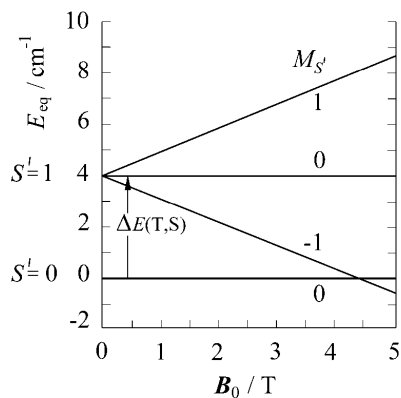

Fig. 2 Correlation diagram of a S_1 = S_2 = 1/2 system under the influence of isotropic intramolecular spin–spin coupling (J_{ex} = –2 cm^{-1}) and applied field.

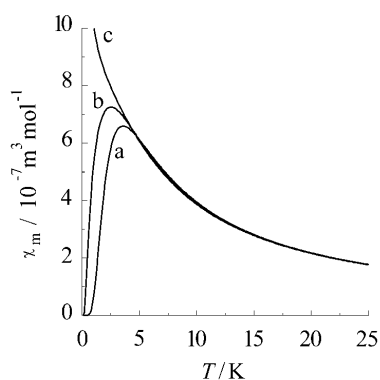**Fig. 3** Calculated variation χ_m vs. T of a $S_1 = S_2 = 1/2$ exchange-coupled system with $J_{ex} = -2$ cm^{-1} at applied fields of $\textbf{\textit{B}}_0 = 0.01$ T (a), 3.5 T (b), and 5 T (c).

a correct adjustment of J_{ex}, either the external field must be weak enough to apply Van Vleck's approach or the susceptibility equation for fitting has to account for the field dependence of the magnetic susceptibility.

4. PRESENTATION OF MEASURED MAGNETIC DATA

Suppose that a new material is available and one wants to get a quick overview on its magnetic properties as a function of temperature and applied field. It is recommended that one run an $\textbf{\textit{m}}(T)$ sweep at low magnetic field ($\textbf{\textit{B}}_0$ in the 10^{-2} T range) over the full temperature range with ΔT steps of 5 K at low temperature and larger steps above it. The weak field guarantees that superconductivity and spontaneous magnetization as well as ferro-/antiferromagnetic couplings and spin cross-over stand out in such a scan. Moreover, regions are identified where μ_{eff} and χ_m vary in a special way with temperature. Then, a complete characterization may follow in the regions of particular interest: (i) under stepwise increase of the applied field ($\Delta \textbf{\textit{B}}_0 \sim 0.5$ T), (ii) performing a zero-field-cooled/field-cooled (ZFC/FC) set of measurements to indicate spontaneously magnetized materials [14–16], (iii) measuring the susceptibility in alternating fields (ac option) to study the dynamics of the magnetic system under investigation [17,18].

To present the temperature-dependent magnetic behavior of paramagnetic samples, the graphs for χ_m^{-1}, μ_{eff}, and χ_m as a function of T are currently used. For magnetically dilute compounds exhibiting Curie paramagnetism, that is, increasing χ_m with decreasing T, the χ_m^{-1}–T plot is especially useful in the case of pure spin magnetism observed for systems with thermally isolated orbital singlet ground states, for example, for both 3d^3, 3d^8 in octahedral surrounding, and 3d^5, 4f^7 ions. They often show a more or less linear behavior. If deviations from linear behavior occur, the μ_{eff}–T plot [19] is reasonable to show the temperature dependence owing to ligand-field effects, including the special feature of spin cross-over [20], as well as cooperative magnetic effects. We recommend one use this plot or alternatively the $\mu_{eff}^2 - T$ plot instead of the $\chi_m T - T$ one for two reasons: (i) The number μ_{eff} has the same numerical value in the SI and CGS-emu system, (ii) μ_{eff} is easily compared with the corresponding spin-only value $\mu_{eff} = 2\sqrt{S(S+1)}$.

Diamagnetism, temperature-independent paramagnetism according to conduction electrons (Pauli paramagnetism), and Van Vleck paramagnetism (TIP) are reasonably presented as $\chi_m - T$ plots.

Ferro- and ferrimagnetic phases ($T < T_C$) are characterized by the variations $\textbf{\textit{M}}_m^*$ vs. $\textbf{\textit{B}}_0$ and $\textbf{\textit{M}}_m$ vs. T. To determine coercivity and remanence, full hysteresis loops in the temperature range of interest

---

*Instead of the molar magnetization $\textbf{\textit{M}}_m$, the atomic magnetic dipole moment μ_a divided by μ_B is a convenient alternative.

are necessary. For $T > T_C$, the $\chi_m^{-1} - T$ plot offers itself. For antiferromagnetic phases, both graphs χ_m^{-1} vs. T and χ_m vs. T are useful regardless of the temperature range above or below the Néel point T_N. To indicate metamagnetic behavior, the variation $\boldsymbol{M}_m$ vs. $\boldsymbol{B}_0$ and its temperature dependence is suitable. Concerning corresponding molecular systems, we refer to ref. [14]. In the case of ferro- and ferrimagnetic interactions, the paramagnetic properties are favorably presented as variation μ_{eff} vs. T. For actual examples, we like to quote ref. [21]. If antiferromagnetic interactions are present, the χ_m vs. T plot is preferred to that of μ_{eff} vs. T one, owing to the indication of a maximum in the magnetic susceptibility and the respective temperature. If occasion arises, their values may serve to evaluate the exchange parameter J_{ex}.

5. INTERPRETATION OF MEASURED DATA

The variation of χ_m, μ_{eff}, $\boldsymbol{M}_m$ vs. T and vs. $\boldsymbol{B}_0$, respectively, serve to characterize the electronic ground state of the magnetic system under investigation. The major effects producing the ground state are interelectronic repulsion (abbreviation H_{ee}), spin-orbit coupling (H_{SO}), ligand field (H_{LF}), interatomic exchange interaction (H_{ex}), and applied magnetic field (H_{mag}). Table 3 gives approximate sizes of the corresponding energy splittings.

Table 3 Effects acting on d and f electrons.

Effect	System	Energy equivalent wavenumber/cm^{-1} [a]
Electron–electron interaction H_{ee}	3d, 4d, 5d	3d > 4d > 5d ≈ 10^4 [b]
	4f, 5f	4f > 5f ≈ 10^4 [b]
Ligand-field potential H_{LF}	3d, 4d, 5d	3d < 4d < 5d ≈ 2×10^4 [b]
	4f	≈ 10^2
	5f	≈ 10^3
Spin-orbit coupling H_{SO}	3d, 4d, 5d	3d < 4d < 5d ≈ 10^3 [b]
	4f, 5f	4f < 5f ≈ 10^3 [b]
Exchange interaction H_{ex}	nd	≤10^2
	4f	<1
	nd–4f	<10
Magnetic field H_{mag}		≈ 0.5 (1 T)

[a]Conversion to other units, see Table 6 (Appendix).
[b]Approximate value according to ref. [22].

5.1 Estimated magnetic behavior of magnetically dilute systems

To predict reliably the magnetic behavior of mononuclear d and f electron systems, computer programs are available [13,23–25]. The general case can be treated considering H_{LF} [26,27] by the angular overlap model [23,28] or the superposition model [27]. If such programs are not at hand, one can estimate the magnetic behavior using the instructions given in Table 4.

Table 4 Overview on the estimated magnetic behavior of d (octahedral ligand field) and f ions (neglecting H_{ex} and H_{mag}).

System	Order of energetic effects	N^a	Ground state	$\chi_m\,(T)^b$
$3d^N$	$H_{ee} \approx H_{LF} > H_{SO}$	5(hs)	$^6A_1$	C/T
		1, 2, 6(hs), 7(hs)	T	$f(T)$
		4(hs), 9	E	$C'/T + \chi_0$
		3, 8	A_2	$C'/T + \chi_0$
	$H_{LF} > H_{ee} > H_{SO}$	6(ls)	$^1A_1$	χ_0
$4d^N$	$H_{LF} > H_{ee} > H_{SO}$			$f(T)$
$5d^N$	$H_{LF} > H_{ee} \approx H_{SO}$			$f(T)$
$4f^N$	$H_{ee} > H_{SO} > H_{LF}$	7	$^8S_{7/2}$	C/T
		1–3, 8–13	$^{2S+1}L_J{}^c$	$f(T)$
		4–6	$^{2S+1}L^d$	$f(T)$
$5f^N$	$H_{ee} > H_{LF} \approx H_{SO}{}^e$			$f(T)$

[a] hs and ls assign high-spin and low-spin configuration, respectively.
[b] $\chi_m = f(T)$ stands for complicated variation χ_m vs. T on account of competing effects; C' is a constant which deviates more or less from the Curie constant C (cf. Table 2) caused by H_{LF} and H_{SO} [29], and χ_0 is a temperature-independent parameter.
[c] Ground multiplet according to Hund's rules.
[d] The full Russell–Saunders term is considered on account of only small splittings by H_{SO}.
[e] For actinide ions in high oxidation states, $H_{ee} \approx H_{LF} \approx H_{SO}$ holds.

For 3d electron systems, the configuration $3d^5$ (high-spin) is outstanding due to the $^6A_1$ ground state which yields the Curie law

$$\chi_m = \frac{C}{T} \qquad \text{with Curie constant} \qquad C = \mu_0\,\frac{N_A\mu_B^2\mu_{eff}^2}{3k_B} \tag{1}$$

corresponding to temperature-independent spin-only μ_{eff}

$$\mu_{eff} = 2\sqrt{S(S+1)} \qquad \text{(spin-only formula)} \quad \text{with} \quad S = 5/2 \tag{2}$$

Another special case is the $^1A_1$ ground state of $3d^6$ low-spin systems leading to temperature-independent (Van Vleck) paramagnetism (TIP) with parabolic variation $\mu_{eff} \sim \sqrt{T}$. In the case of a non-half-filled 3d subshell, the ground state can be A, E, or T. For the former two, χ_m is often given as a sum of a temperature-dependent Curie term and a TIP contribution χ_0 (see Table 4) where μ_{eff} is close to the spin-only value and varies only a little with temperature. The μ_{eff} behavior of systems with T ground terms, however, is strongly temperature-dependent [29,30]. As an example, the variation μ_{eff} vs. T and χ_m^{-1} vs. T of a $3d^1$ ion, e.g., Ti^{3+}, V^{4+}, is exhibited in Fig. 4 where the ligand field has octahedral and orthorhombic symmetry, respectively. For the octahedral system, the unquenched orbital contribution to the magnetic moment and the spin part produce via H_{SO} a nonmagnetic ground state ($\mu_{eff} \to 0$ for $T \to 0$). The variation χ_m^{-1} vs. T shows another feature in that for $T > 150$ K a linear increase with temperature is observed. Reducing further the ligand field symmetry, for example, to C_{2v}, the quenching of orbital contributions to μ_{eff} is (nearly) complete so that H_{SO} has no effect. Almost pure spin magnetism results with a temperature-independent $\mu_{eff} = 1.73$.

In 4d and 5d electron systems, H_{SO} increases and H_{ee} decreases compared to the 3d case. No simple formula is available to describe the variation μ_{eff} vs. T. As a rule, the μ_{eff} values are lower than those of comparable 3d systems.
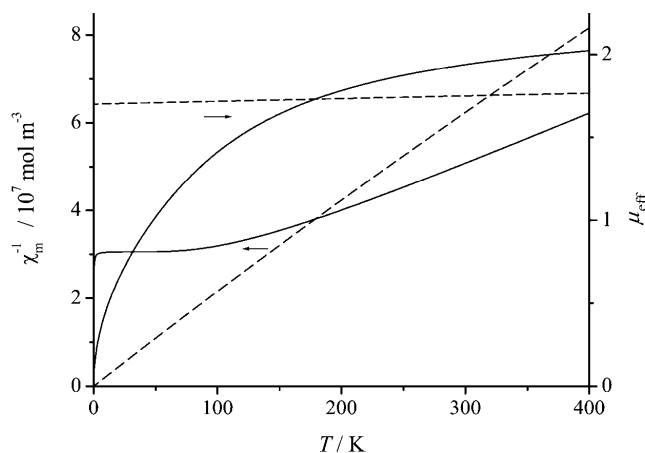
Fig. 4 Calculated variation of μ_{eff} vs. T and χ_m^{-1} vs. T plots of a 3d^1 ion in octahedral (——) and orthorhombic (– – –) surrounding.

The magnetic behavior of 4f electron systems is well predictable with programs [13,23]. Neglecting the influence of the ligand field, which means temperatures well above 100 K, and having a magnetic ground state of specific J, Hund's formula applies:

$$\mu_{eff} = g_J \sqrt{J(J+1)} \quad \text{with } g_J = 1 + \frac{J(J+1) + S(S+1) - L(L+1)}{2J(J+1)} \tag{3}$$

It is recommended that one display a graph showing the variation μ_{eff} vs. T. Because of Kramers' rule for centers with an odd number of 4f electrons, a degenerate ground state is always observed leading to Curie behavior at temperatures below 10–20 K (in the absence of magnetic cooperative effects). In the case of an even number of f electrons, degenerate as well as nondegenerate ground states can be found leading to Curie behavior and TIP, respectively, at low temperature.

Going to 5f electron systems, H_{SO} and H_{LF} increase according to the larger effective nuclear charge and the fact that 5f electrons are more accessible for ligands, respectively. No simple approximation can be made. So, the only possibility to predict the magnetic behavior for the ions are computational methods [13,23].

5.2 Estimated magnetic behavior of magnetically condensed systems

If the magnetic susceptibilities, recorded at low applied fields, cannot be explained by the above-mentioned laws and if corresponding structural reasons are given, exchange effects possibly have to be included. For such systems showing cooperative magnetic phenomena like antiferro- or ferromagnetic interactions, the following methods can be applied for the interpretation of the magnetic behavior.

For half-filled subshell systems [Mn^{2+}(hs), Fe^{3+}(hs), Eu^{2+}, Gd^{3+}] where ligand field effects play no role, the aforementioned methods lead to the spin-only formula with Curie behavior. Deviations from this behavior are due to cooperative effects which can be described at sufficiently high temperature with the Curie–Weiss law

$$\chi_m = \frac{C}{T - \theta} \quad \text{with } \theta = \frac{2S(S+1)}{3k_B} \sum_i^n z_i J_{ex,i}, \tag{4}$$

where θ is the Weiss constant; z_i is the number of ith nearest neighbors of a given magnetic center, $J_{ex,i}$ stands for the exchange interaction between the ith neighbors, and n is the number of sets of neighbors

for which $J_{ex,i} \neq 0$ [31]. Positive and negative θ values refer to predominating ferro- and antiferro-magnetic interactions, respectively. The layer-type compound $FeCl_2$ may serve as an example that is magnetically characterized by dominating ferromagnetic intralayer and weaker antiferromagnetic inter-layer interactions. This does lead to $\theta > 0$, but an antiferromagnetic spin structure is observed below the Néel temperature. In such extended magnetic systems, a classification of the interactions with respect to nearest, next-nearest, and further neighbors is possible if the susceptibility data at temperatures between the Curie–Weiss region and the magnetic ordering temperature (T_C, T_N) are included in fitting procedures on the basis of a powerful approach, the high-temperature series expansion [6,32,33].

Unfortunately, the Curie–Weiss law is also often used for magnetically dilute systems, misinter-preting the effect of $H_{LF} + H_{SO}$ as cooperative phenomena. For instance, it is possible to describe roughly the variation χ_m^{-1} vs. T of the $3d^1$(oct.) system at $T > 150$ K by this law (see Fig. 4). However, cooperative magnetic effects are excluded and the corresponding "θ" value is meaningless in this re-spect. Similarly, attempts to fit the paramagnetic properties of f systems (except for $4f^7$ configuration) on the basis of the Curie–Weiss law are not justified (see ref. [34] for a deeper discussion).

For nonhalf-filled subshells where both exchange and ligand field effects play a major role and where the single ion behavior deviates from Curie law, the variation of the magnetic susceptibility with temperature above the ordering temperature is described by the molecular field model in the form

$$\chi_m^{-1} = \left(\chi_m^{'} \right)^{-1} - \lambda \quad \text{with} \quad \lambda = \frac{2\sum_i^n z_i J_{ex,i}}{\mu_0 N_A \mu_B^2 g^2} \tag{5}$$

where χ'_m refers to the single ion susceptibility and the molecular field parameter λ describes the ex-change interactions in the molecular field model; g may deviate more or less from 2, depending on or-bital contributions to the center's magnetic moment.

Finally, we emphasize so-called high-nuclearity magnetic clusters. These entities are the object of an essential and fast-growing field in molecular magnetism. Advanced computer programs have been developed for the interpretation of the characteristic magnetic features of such systems [35].

5.3 Hints on publication of magnetochemical results

If magnetochemical results are to be published, it is recommended that one give the following infor-mation: (i) magnetometer, magnetic field strength, temperature range; (ii) diamagnetic correction; (iii) number of magnetic centers to which the measured quantities refer [36]; and (iv) definition of the ex-change parameter $J_{ex,i}$ in the form of the relevant spin hamiltonian. Unfortunately, $J_{ex,i}$ is not uniformly defined. Instead of the original version $\hat{H}_{ex} = -2J_{ex} \hat{S}_1 \cdot \hat{S}_2$ [4,5] preferred by us, one finds $\hat{H}_{ex} = -J_{ex} \hat{S}_1 \cdot \hat{S}_2$ [14] and $\hat{H}_{ex} = J_{ex} \hat{S}_1 \cdot \hat{S}_2$ [21]. Furthermore, most authors do give J_{ex} in units of cm^{-1}, but K and eV are also in use (see Appendix, Table 6 for conversion factors). Sometimes, this may be a problem in the development of magneto-structural correlations, if several series of J_{ex} values, obtained by different authors, are to be compared.

ACKNOWLEDGMENTS

REFERENCES

1. Information on SQUID magnetometers can be found at <http://hyperphysics.phy-astr.gsu.edu/-hbase/solids/squid.html>.

2. IUPAC. *Quantities, Units and Symbols in Physical Chemistry* (the "Green Book") 2nd ed., prepared for publication by I. Mills, T. Cvitaš, K. Homann, N. Kallay, K. Kuchitsu, Blackwell Science, Oxford (1993); see especially sections 2.3, 7.2, 7.3, 7.4.

3. T. I. Quickenden and R. C. Marshall. *J. Chem. Educ.* **49**, 114 (1972).

4. B. I. Bleaney and B. Bleaney. *Electricity and Magnetism*, 3rd ed., Oxford University Press, Oxford (1994).

5. J. H. Van Vleck. *Electric and Magnetic Susceptibilities*, Oxford University Press, Oxford (1932).

6. H. Lueken. *Magnetochemie*, Teubner, Stuttgart (1999).

7. D. Nelson and L. W. ter Haar. *Inorg. Chem.* **32**, 182 (1993).

8. A. H. Cooke. In *Prog. Low Temp. Phys.,* C. J. Gorter (Ed.), **1**, 224 (1955).

9. G. K. White. *Experimental Techniques in Low-temperature Physics,* Clarendon Press, Oxford (1993).

10. L. D. Swartzendruber. *J. Magn. Magn. Mater.* **100**, 573 (1991).

11. The condition $\mu_a^s B_0/k_B T \ll 1$ is valid for the initial linear part of the Brillouin function where μ_a^s is the atomic magnetic saturation moment given by $g_J J \mu_B$ (cf. eq. 3) and $g S \mu_B$ with $g = 2$ for the ground state of a free lanthanide ion and an ion with spin-only magnetism, respectively.

12. $\mu_{eff} = 8.94$ is obtained according to $\mu_{eff} = 2\sqrt{S'(S'+1)}$ with $S' = 7/2 + 1/2$ for the ferromagnetically coupled Gd–Cu unit. If the ions are uncoupled, $\mu_{eff} = 8.13$ is achieved according to $\mu_{eff} = \sqrt{\mu_{eff}^2 (Gd) + \mu_{eff}^2 (Cu)}$ with $\mu_{eff} (Gd) = 7.94$ and $\mu_{eff} (Cu) = 1.73$.

13. H. Schilder and H. Lueken. *J. Magn. Magn. Mater.* **281**, 17 (2004); PROGRAM CONDON is free software, covered by the GNU General Public Licence, and is available from <http:// www.condon.fh-aachen.de>.

14. O. Kahn. *Molecular Magnetism*, Wiley-VCH, New York (1993).

15. E. Coronado, P. Delhaès, D. Gatteschi, J. S. Miller (Eds.). *Molecular Magnetism: From Molecular Assemblies to the Devices*, NATO ASI Series, Series E: Applied Sciences, Vol. 321, Kluwer, Dordrecht (1996).

16. M. McElfresh. *Fundamentals of Magnetism and Magnetic Measurements*, Quantum Design, San Diego (1994).

17. R. L. Carlin. *Magnetochemistry*, Springer, Berlin (1986).

18. W. M. Reiff. Magnetic Susceptibility Measurements: An Important Facet of Modern Solid-State Characterization, *International Laboratory*, 28 (1994).

19. As an alternative, $\mu_{eff}^2 \sim \chi_m T$ can be used with the advantage that μ_{eff}^2 reflects the temperature dependence more sensitively than μ_{eff}.

20. (a) P. Gütlich, A. Hauser, H. Spiering. *Angew. Chem., Int. Ed.* **33**, 2024 (1994); (b) E. Breuning, M. Ruben, J.-M. Lehn, F. Renz, Y. Garcia, V. Ksenofontov, P. Gütlich, E. Wegelius, K. Rissanen. *Angew. Chem. Int. Ed.* **39**, 2504 (2000).

21. D. Gatteschi and R. Sessoli. *Angew. Chem., Int. Ed.* **42**, 268 (2003).

22. A. F. Williams. *A Theoretical Approach to Inorganic Chemistry*, Springer, Berlin (1979).

23. (a) W. Urland. *Chem. Phys.* **14**, 393 (1976); (b) W. Urland. *Chem. Phys. Lett.* **46**, 457 (1977).

24. M. Gerloch. *Magnetism and Ligand-field Analysis,* Cambridge University Press, Cambridge (1983).

25. H. Adamsky, M. Atanasov, T. Schönherr. In *Comprehensive Coordination Chemistry II, From Biology to Nanotechnology*, Vol. 1: Fundamentals, 1.98 The AOMX Program, T. J. Meyer and J. A. McCleverty (Eds.), Elsevier, Amsterdam (2003/2004).

26. C. Görller-Walrand and K. Binnemans. In *Handbook on the Physics and Chemistry of Rare Earths*, Vol. 23, K. A. Gschneidner and L. Eyring (Eds.), Chap. 155, Elsevier, Amsterdam (1996).

27. D. J. Newman and B. K. C. Ng (Eds.). *Crystal Field Handbook*, Cambridge University Press, Cambridge (2000).

28. C. E. Schäffer and C. K. Jørgensen. *Mol. Phys.* **9**, 401 (1965).

29. F. E. Mabbs and D. J. Machin. *Magnetism and Transition Metal Complexes*, Chapman and Hall, London (1973).
30. J. S. Griffith. *The Theory of Transition-Metal Ions*, Cambridge University Press, Cambridge (1971).
31. J. S. Smart. *Effective Field Theories of Magnetism*, Saunders, Philadelphia (1966).
32. G. S. Rushbrooke and P. J. Wood. *Mol. Phys.* **1**, 257 (1958).
33. (a) Th. Eifert, F. Hüning, H. Lueken, P. Schmidt, G. Thiele. *Chem. Phys. Lett.* **364**, 69 (2002); (b) Th. Eifert, software 'HTSE Package', RWTH Aachen (2001). Available from: <http://www.rz.rwth-aachen.de/eifert/information/HTSE>.
34. J. H. Van Vleck. *Physica* **69**, 177 (1973).
35. (a) D. Gatteschi and L. Pardi. *Gazz. Chim. Acta* **123**, 231 (1993); (b) J. J. Borrás-Almenar, J. M. Clemente-Juan, E. Coronado, B. S. Tsukerblat. *Inorg. Chem.* **38**, 6081 (1999).
36. Magnetic quantities per magnetically active center should be given to achieve valid comparisons among different sets of data.
37. K.-H. Hellwege. *Einführung in die Festkörperphysik*, Springer, Berlin (1988).

APPENDIX: ENERGY EQUIVALENTS AND ENERGY CONVERSION FACTORS

For the energy E, the following relations hold:

$$E = h\nu = hc_0\tilde{\nu} = k_\mathrm{B}T = \underbrace{\left(e\hbar/2m_\mathrm{e}\right)|\boldsymbol{B}|}_{\mu_B|\boldsymbol{B}|} = E_\mathrm{m}/N_\mathrm{A}$$

with h the Planck constant, c_0 the speed of light in vacuum, k_B the Boltzmann constant, m_e the electron rest mass, e the elementary charge, $\hbar = h/2\pi$, μ_B the Bohr magneton, and N_A the Avogadro constant.

Energy equivalents, labeled by subscript 'eq' on the symbol E, are physical quantities that, when multiplied or divided by one or more fundamental physical constants (cf. Table 5), yield quantities that have dimensions of energy. The energy equivalents E_eq (with their SI units) are given in terms of

frequency	$E_\mathrm{eq} = E/h = \nu$	s^{-1}
wavenumber	$E_\mathrm{eq} = E/hc_0 = \tilde{\nu}$	cm^{-1}
temperature	$E_\mathrm{eq} = E/k_\mathrm{B} = T$	K
magnitude of magnetic induction	$E_\mathrm{eq} = E/\mu_\mathrm{B} = |\boldsymbol{B}|$	T
molar energy	$E_\mathrm{eq} = E N_\mathrm{A} = E_\mathrm{m}$	$\mathrm{kJ\ mol}^{-1}$

Table 5 Physical constants.

Symbol		SI	CGS-emu
h	Planck constant	$6.626\ 07 \times 10^{-34}$ J s	$6.626\ 07 \times 10^{-27}$ erg s
k_B	Boltzmann constant	$1.380\ 66 \times 10^{-23}$ J/K	$1.380\ 66 \times 10^{-16}$ erg/K
μ_B	Bohr magneton	$9.274\ 02 \times 10^{-24}$ A m^2	$9.274\ 02 \times 10^{-21}$ G cm^3
c_0	Speed of light in vacuum	$2.997\ 924\ 58 \times 10^8$ m/s	$2.997\ 924\ 58 \times 10^{10}$ cm/s
m_e	Electron rest mass	$9.109\ 39 \times 10^{-31}$ kg	$9.109\ 39 \times 10^{-28}$ g
N_A	Avogadro constant	$6.022\ 14 \times 10^{23}$ mol^{-1}	
e	Elementary charge	$1.602\ 18 \times 10^{-19}$ C	

Table 6 gives numerical values of the energy equivalents. Conversion to electronvolt (eV) is straightforward, and does not involve an energy equivalent.

Table 6 Energy conversion factors (after [37]).

		E		E_{eq}				
		J	eV	s^{-1}	cm^{-1}	K	T	kJ mol^{-1}
E	1 J =	1	$6.241\ 51 \times 10^{18}$	$1.509\ 19 \times 10^{33}$	$5.034\ 11 \times 10^{22}$	$7.242\ 92 \times 10^{22}$	$1.078\ 28 \times 10^{23}$	$6.022\ 14 \times 10^{20}$
	1 eV =	$1.602\ 18 \times 10^{-19}$	1	$2.417\ 99 \times 10^{14}$	$8.065\ 54 \times 10^{3}$	$1.160\ 45 \times 10^{4}$	$1.727\ 60 \times 10^{4}$	$9.648\ 53 \times 10^{1}$
E_{eq}	1 s^{-1} =	$6.626\ 07 \times 10^{-34}$	$4.135\ 67 \times 10^{-15}$	1	$3.335\ 64 \times 10^{-11}$	$4.799\ 22 \times 10^{-11}$	$7.144\ 77 \times 10^{-11}$	$3.990\ 31 \times 10^{-13}$
	1 cm^{-1} =	$1.986\ 45 \times 10^{-23}$	$1.239\ 84 \times 10^{-4}$	$2.997\ 92 \times 10^{10}$	1	$1.438\ 77$	$2.141\ 95$	$1.196\ 26 \times 10^{-2}$
	1 K =	$1.380\ 66 \times 10^{-23}$	$8.617\ 39 \times 10^{-5}$	$2.083\ 67 \times 10^{10}$	$6.950\ 39 \times 10^{-1}$	1	$1.488\ 74$	$8.314\ 51 \times 10^{-3}$
	1 T =	$9.274\ 02 \times 10^{-24}$	$5.788\ 39 \times 10^{-5}$	$1.399\ 63 \times 10^{10}$	$4.668\ 64 \times 10^{-1}$	$6.717\ 10 \times 10^{-1}$	1	$5.584\ 94 \times 10^{-3}$
	1 kJ mol^{-1} =	$1.660\ 54 \times 10^{-21}$	$1.036\ 42 \times 10^{-2}$	$2.506\ 07 \times 10^{12}$	$8.359\ 33 \times 10^{1}$	$1.202\ 72 \times 10^{2}$	$1.790\ 53 \times 10^{2}$	1